Thermotropic mesomorphism of cholesteryl myristate. An electron diffraction study

Douglas L. Dorset

Electron Diffraction Department, Medical Foundation of Buffalo, Inc., 73 High Street, Buffalo, NY 14203

Abstract Electron diffraction measurements on heated or cooled microcrystals of cholesteryl myristate, which are grown from solution or epitaxially, on benzoic acid, provide further structural information about its mesomorphic behavior. At subambient temperatures ($< -65°C$), a new crystal form is observed which doubles the unit cell axes in the (001) plane. At the major crystalline ⇌ smectic endotherm at 70°C, evidence is found for the existence of a pretransition crystal packing. The smectic phase, which coexists with this pretransition crystal form, is composed of relatively well-ordered layers, probably with a monolayer-type packing. Cooling the cholesteric phase to the crystalline form causes a rotational disorder which is not yet understood. — **Dorset, D. L.** Thermotropic mesomorphism of cholesteryl myristate. An electron diffraction study. *J. Lipid Res.* 1985. **26:** 1142–1150.

Supplementary key words crystalline • smectic • cholesteric

Cholesteryl myristate, which forms at least two separate liquid crystalline phases before it melts (1) [and at least two so-called "blue phases" in the higher temperature cholesteric (2–5)], is one of the most studied of mesogenic compounds. The liquid crystalline transitions in the following scheme: crystalline ⇌ smectic ⇌ cholesteric ⇌ melt, have been found by measurements of various physical properties (6–10) to be more or less enantiotropic. Attempts to characterize the structural changes with X-ray (11–13) and neutron (14) powder diffraction techniques, however, have been only partially successful, even though these transitions can now be compared to the complete single crystal X-ray structure (15).

Most of the difficulty in interpreting powder diffraction data is caused by the random orientation of the bulk sample. Electron diffraction patterns on individual thin microcrystals, on the other hand, enable the characterization of structural transition in terms of an oriented crystal lattice, as has been shown recently in a study of the premelt transition of n-paraffins (16). In such study of molecular organics containing alkane chains, use can also be made of epitaxial growth techniques in addition to the normally employed solution growth to provide two orthogonal views of the crystal packing (17).

In the current view of molecular packing in the smectic phase of cholesteryl myristate, at least two different models have been suggested that alternatively accept (12) or reject (15) the notions of molecular interpenetration, i.e., a packing scheme that would surround cholesterol steroid nuclei with acyl chains. As will be discussed in this communication, new electron diffraction data can be adduced in favor of the interpenetrated structure model. Such data also demonstrate, for the first time, the presence of pre-transition crystal packing that coexists with the smectic phase, in agreement with earlier thermal measurements.

MATERIALS AND METHODS

Crystallization

Cholesteryl myristate (Sigma Chemical Co., St. Louis, MO) was recrystallized as thin microplatelets from n-pentanol onto carbon film-covered copper electron microscope grids for electron diffraction studies of the "solution crystallized" form. Epitaxial crystallization was carried out by successive melting and cooling of a dilute solution of the cholesteryl ester in benzoic acid between two mica plates, according to the procedure of Wittmann, Hodge, and Lotz (18) for paraffins and linear polymers.

Electron diffraction and microscopy

Electron diffraction experiments on microcrystalline preparations were carried out at 100 kV using a JEOL JEM-100B (JEOL USA, Inc., Peabody, MA) electron microscope, ensuring that beam damage to the specimen was minimized by: *a*) low incident beam current density and *b*) fast photographic emulsions to record the diffraction patterns (here Kodak DEF-5 X-ray film (Eastman Kodak Co., Rochester, NY)). Diffraction pattern spacings were calibrated with a gold powder sample deposited in vacuo onto representative specimen grids. Initial visualizations of crystal texture were made via low dose, low magnification (6.7×10^3) bright field diffraction contrast images of the specimen. Later, higher resolution images

were obtained at room temperature to visualize the lamellar spacing in reference to the crystal habit. In this work the microscope was first aligned at 170,000 × (including correction for objective lens astigmatism) and low dose images of the specimen recorded later on DEF5 X-ray film at a working magnification of 17,000 ×. Using the deliberately misaligned redundant "dark field" condenser lens controls as a shutter, the exposures to the specimen were therefore controlled such that a focal series of three micrographs could be recorded without substantial change in the electron diffraction pattern due to radiation damage. Areas of suitable micrographs were then evaluated via optical transforms on an optical bench with He-Ne laser light source (Polaron Instruments, Inc., Hatfield, PA). For heating/cooling experiments, a Gatan Model 626 specimen stage (Gatan Inc., Warrendale, PA) capable of holding temperatures from −170° to +150°C was inserted into the side entry goniometer stage of the electron microscope.

Calculations

Quantitative interpretation of electron diffraction intensities (experimentally obtained by integration of scans made by a Joyce Loebl MkIIIC (Joyce Loebl & Co., Ltd., Gateshead on Tyne, England) flat bed microdensitometer) require corrections for two major perturbations to these data. Particularly important for solution-grown crystals of long chain compounds is a correction for the apparent diffraction incoherence caused by elastic crystal bending, as discussed by Cowley (19) and other workers (20, 21), i.e.,

$$I(\vec{s}) = \sum_i W_i(\vec{s})\exp(2\pi i \vec{r}_i \cdot \vec{s})\exp(-\pi^2 c^2 s^2 z_i^2).$$

The observed diffraction intensities $I(\vec{s})$ are treated as the Fourier transform of the Patterson function with peak form factors $W_i(s)$ that are modulated by a Gaussian smearing term which contains: the amount of crystal bending c in radians, the reciprocal distance of a particular reflection $|s| = d^*$, and the z component of the unit cell length in the beam direction.

In addition, the electron diffraction intensities from thick crystals are altered by n-beam dynamical scattering. Since this correction is most important for a limited number of low angle data from epitaxially crystallized specimens, we have used a phase-grating calculation of the structure factor magnitudes (22), i.e.,

$$F_{hk}^{dyn} = \mathcal{F}(q(x,y)) = \mathcal{F}\exp[-i\sigma t\phi(x,y)]$$

instead of a rigorous multislice dynamical calculation. In this expression q(x,y) is the propagation function for a crystal slice of thickness t and $\phi(x,y)$ is the electrostatic potential distribution in that slice. The term

$$\sigma = \frac{2\pi}{\lambda \cdot W[1+(1-\beta^2)^{1/2}]}$$

is the so-called interaction constant which includes the electron wavelength λ.

Other crystallographic programs include variants of standard structure factor computations that allow use of non-integral Miller indices for calculation of continuous Fourier transforms. In all of these computations, Doyle-Turner (23) electron scattering factors were employed.

RESULTS

Structural characterization

Subambient crystal form. Solution-crystallized samples of cholesteryl myristate give transmission electron diffraction patterns as shown in **Fig. 1a,** while those crystallized epitaxially on benzoic acid diffract as shown in **Fig. 2a.** (As discussed in the next section these patterns represent two orthogonal projections of the same crystal structure.) Between −65°C and −70°C, there is a doubling of the diffraction spacings and, sometimes, a streaking of peaks along a^* (Fig. 1b). The former indicates a structural transition and the latter perhaps a "cigarello"-type microtwinning that would produce such streaks (24). Electron diffraction patterns from epitaxially crystallized specimens (Fig. 2a), on the other hand, reveal no difference in specimens cooled to −164°C. Thus, the change in crystal structure due to cooling is directional.

Crystalline ⇌ smectic transition. Transmission electron diffraction intensities from solution-crystallized samples agree well with the known crystal structure after these data are corrected for observed elastic crystal bending, as shown in **Table 1.** Lamellar data from epitaxially crystallized samples likewise agree with the crystal structure after correction for dynamical scattering from rather thick (e.g., 265 Å) crystal plates (see **Table 2**). However, unlike the case with other long chain materials, it is difficult to say at first what projection of the crystal structure is epitaxially nucleated by the benzoic acid substrate. Measurement of interplanar reciprocal spacings normal to the lamellar reflections (see Fig. 2a) give values coincident with the (010), (110), (200), (210), and (020) reflection positions in the X-ray crystal structure (15), indicating disorder around the long axis. Such disorder is found to a greater or lesser degree in epitaxial crystals of other long chain materials (25). The b = 5.14 Å spacing in the largest crystal face of benzoic acid (18) would easily account for the nucleation of the (010) projection of the ester, since the respective spacings of steroid nuclei and alkyl chains of 9.9 Å and 4.9 Å correspond well to this value (or its double). The alternative nucleation of the (100) crystal face is less easy to imagine and could only be achieved by a match of 2 × (b = 7.69 Å) ester spacing to the 3 × 5.14 Å spacing of benzoic acid and thus would be discounted if the 01ℓ and 02ℓ reciprocal lattice rows were not observed in the electron diffraction pattern. Further-

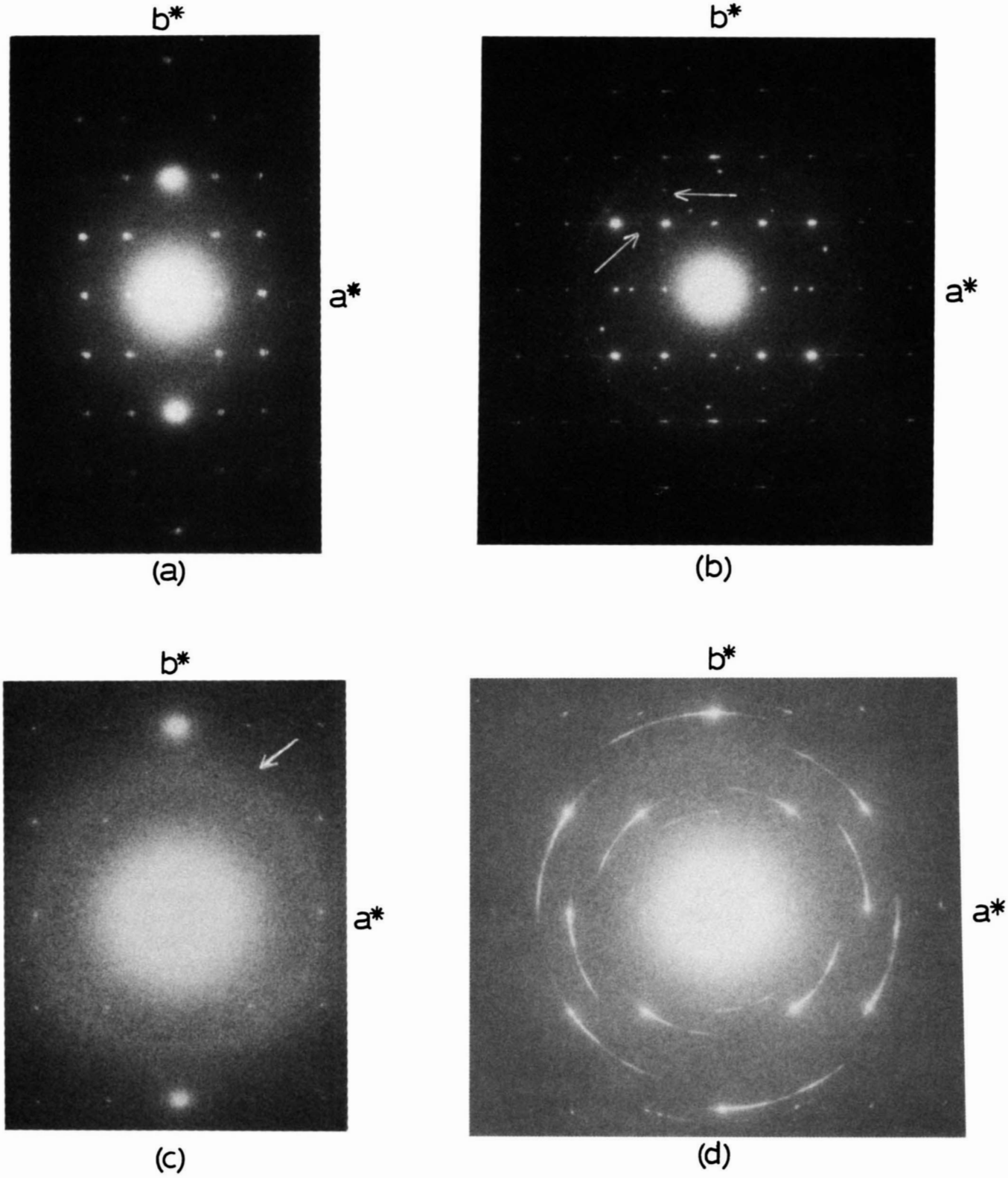

Fig. 1. Transmission electron diffraction patterns from thin solution crystallized samples of cholesteryl myristate. (a) Room temperature crystal form: d_{100} = 10.36 ± 0.10 Å, d_{010} = 7.68 ± 0.06 Å (compare to values given by Craven and DeTitta (15): a = 10.26, b = 7.596, c = 101.45 Å, β = 94.41°); (b) low temperature form (< −65°C): d_{100} = 20.84 ± 0.12 Å, d_{010} = 15.36 ± 0.12 Å; note the presence of a superimposed diffraction pattern from an adjacent crystal. Reflections that denote the doubling of unit cell axes are indicated by arrows; (c) transition to the smectic; note superposition of the crystalline hk0 pattern on the diffuse ring at 5.0 Å; (d) rotational disorder in the hk0 pattern when the specimen is cooled from the cholesteric phase (but not the smectic phase).

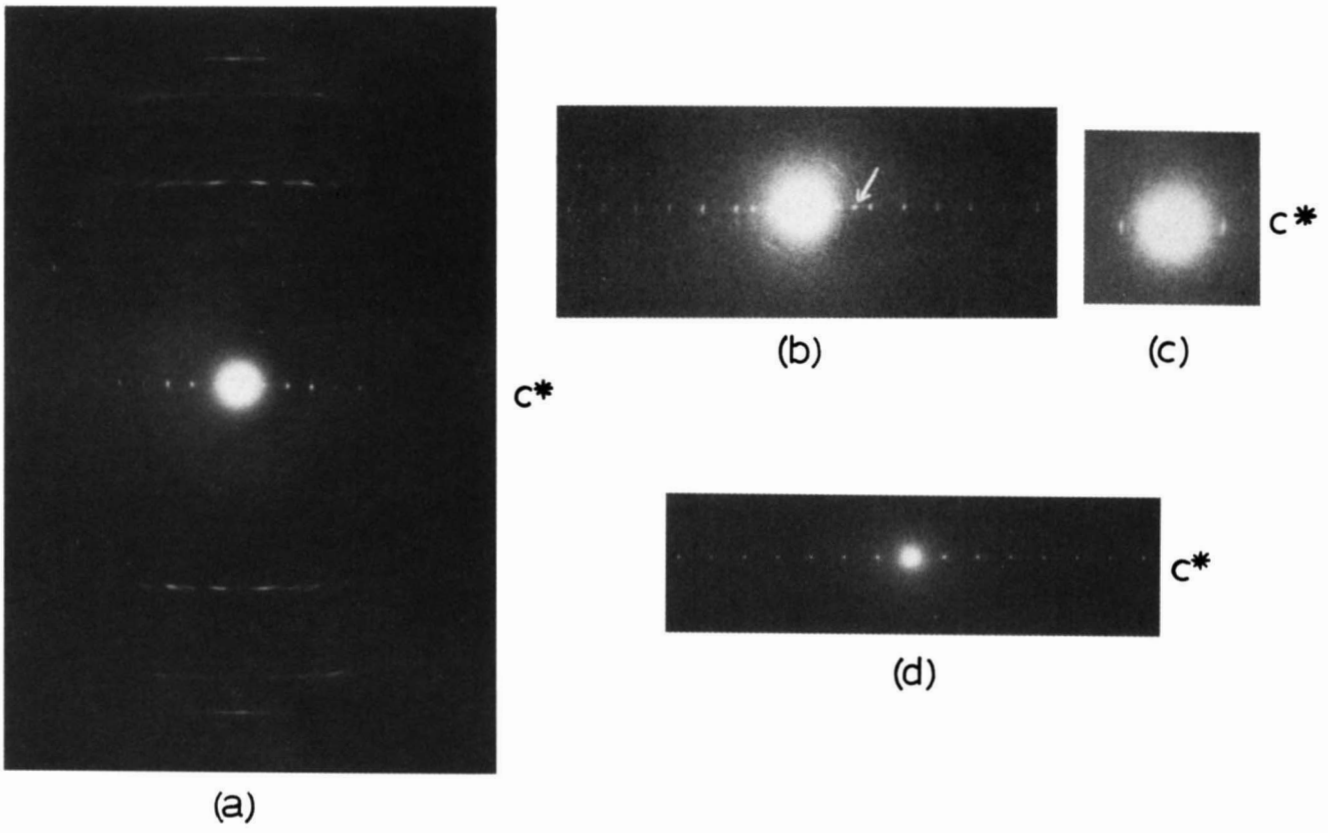

Fig. 2. Transmission electron diffraction patterns from epitaxially crystallized specimens of cholesteryl myristate. (a) Room temperature and subambient structure: ½ $d_{00\ell}$ = 50.58 ± 0.59 Å. As with many epitaxially crystallized materials (17) there is rotational disorder about c*; (b) pretransition to the smectic phase (68°C). Note the superposition of a sharp spot at d = 33.19 Å on the crystalline 00ℓ row. Note the change of relative 00ℓ reflection intensities and also their increased sharpness; (c) smectic diffraction pattern seen above 70°C; (d) diffraction pattern from a specimen cooled from the smectic phase.

more, nucleation of this latter zone requires an oblique packing of the molecules to the aromatic substrate crystal face (ca. 15.6°) if the cholesteryl ester retains crystal faces defined by the X-ray crystal structure. If these faces are not retained and the molecules lie flat on the substrate to give a new (100) projection, the lamellar intensities are changed. Comparison of structure factors for such a projection to observed data in fact give a poorer match to observed data than those of the X-ray crystal structure (Table 2). It is therefore concluded that the nucleation occurs on (010) for cholesteryl myristate which gives a best fit of molecules with the (001) plane of benzoic acid and also allows growth of an oblique layer in the plane. As shown by structure factor calculations, the two zones produced, respectively, by solution growth and epitaxy are orthogonal views of the same crystal structure. The reason for rotational disorder in the epitaxial crystals, which limits us to the use of lamellar data for quantitative structure analyses, is not fully understood even though low dose lattice images of the crystal texture (**Fig. 3**) indicate that elastic bending causes significant areas of the crystal to be oriented away from the (010) projection.

Although the phase transition produces some molecular reorientation, there is no a/b axial ratio change in diffraction patterns heated to 68°C. For solution-grown samples there is an occasional superposition of the crystalline hk0 pattern in the diffuse 5.0 Å ring at 68°C (Fig. 1c). The most salient changes are seen in the epitaxially crystallized material. At 68°C the smectic phase pattern is often superimposed on the crystalline 00ℓ pattern, i.e., a sharp diffraction spot with $(33\ \text{Å})^{-1}$ spacing appears in the crystalline reciprocal lattice row spaced at $(50.6\ \text{Å})^{-1}$; this demonstrates that the smectic lamellae have the same orientation as the crystalline layers (Fig. 2b) and also that there is no measurable change in the *crystal* c-spacing.

There is also a change in 00ℓ crystal diffraction intensities near 68°C, indicating a new crystalline packing (Fig. 2b). Although claims of such intensity changes must be made cautiously in electron diffraction experiments (owing to the other possible data perturbations indicated above), justification of this change is based on the following. First, the observed 00ℓ intensities from several samples in this pretransition crystal phase are similar, giving an average crystallographic residual 0.22 ± 0.10,

TABLE 1. Comparison of observed hk0 structure factors to the known crystal structure, corrected for elastic crystal bending

hk0	$\|F_{obs}\|$	$\|F_{calc}\|$ 0° Bend	$\|F_{calc}\|$ 2.5° Bend
010	0.21	0	0.39
020	1.49	2.94	1.46
030	0.00	0	0.08
040	0.55	0.59	0.35
050	0.00	0	0.05
060	0.29	0.32	0.10
100	0.23	0.45	0.57
110	0.35	0	0.50
120	0.32	0.46	0.45
130	0.31	0	0.32
140	0.22	0.21	0.15
150	0.25	0	0.11
160	0.20	0.05	0.07
200	0.45	0.82	0.52
210	0.37	0	0.52
220	0.27	0.41	0.20
230	0.32	0	0.31
240	0.18	0.11	0.13
250	0.24	0	0.11
260	0.24	0.14	0.09
R		0.73	0.36[a]

$$R = \frac{\Sigma \left| |F_{obs}| - k|F_{calc}| \right|}{\Sigma |F_{obs}|}$$

[a]Lowest value for another data set R = 0.29.

which demonstrates overall consistency of the data. Second, these changes cannot be explained in terms of dynamical scattering since the intensity data agree neither with those from unheated crystals nor with theoretical intensities obtained from a dynamical calculation (the average residual is now 0.64 ± 0.09). On cooling, the altered crystal structure persists, but the previous crystal form slowly reappears. One also notes a sharpening of all diffraction spots in this pretransition structure which persists after cooling (Fig. 2d), but is not itself caused by cooling the specimen. Optical transforms (Fig. 3b) of the images, which permit the sampling of smaller areas than permitted by selected area diffraction, however, indicate that individual crystallites are well ordered below this pretransition; the heating merely fuses adjacent crystallites into a larger well-oriented crystal. Above the transition to the smectic phase, only a Friedel doublet of spots remains (Fig. 2c).

Smectic ⇌ cholesteric transition. Very little direct information could be obtained about the cholesteric phase from electron diffraction data. Solution-grown samples give the diffuse diffraction ring at 5.0 Å seen also in the smectic phase. Although the 33 Å diffraction peak is found for epitaxial samples in the smectic phase, it is never seen in the cholesteric phase, contrary to previous X-ray diffraction measurements. This may be due to a rearrangement of the original crystal texture, so that the molecular axes are now directed normal to the crystal surface. Alternatively, there may have been residual smectic phase in the bulk sample examined in the original powder X-ray study (12).

There have been differences observed in specimens cooled to the crystalline phase, respectively, from the smectic and cholesteric phase. Diffraction patterns in the first case retain their order, but those from specimens cooled from the cholesteric indicate a rotational disorder of the specimen (Fig. 1d).

DISCUSSION

Many of the inconsistencies noted for the thermal behavior of cholesteryl myristate have been shown by previous workers (6-9) to be due to well-known kinetic processes that can retard the recrystallization of a disordered sample. The subambient transition, which has been classified (8) as H in the Westrum-McCullough (26) notation for plots of Cp versus T, is a case in point, and is undoubtedly a minor change in the crystal structure that may lead to thin lath-like polarized crystal sections along the *a* axis which alternate in a microtwin arrangement, broadening the diffraction peaks with an average Ewald shape function (24). Since the cholesterol isoprenoid side chain has the largest thermal motion in the crystal structure (15) and since cooling greatly increases the resolution of the hk0 diffraction data, this may be due to two alternative crystallization modes for this moiety.

Obviously, kinetic factors are also important in the largest endotherm, noted in calorimetric measurements, which is classified 2I, denoting the importance of pretransition changes in the crystal structure (8), which can persist even in specimens cooled in liquid nitrogen. It is not easy to characterize the structure changes that accompany this transition and also the subsequent change to the smectic phase, which gives only one diffraction

TABLE 2. Comparison of observed 00*ℓ* structure factors to the known crystal structure model (assuming steroid ring nucleation). Dynamical correction for 265 Å crystal thickness

00*ℓ*	$\|F_{obs}\|$	$\|F_{calc}\|$
002	0.63	0.65
004	1.14	1.50
006	1.14	1.09
008	0.33	0.23
0010	0.48	0.42
0012	0.29	0.11
0014	0.00	0.09
0016	0.28	0.18
0018	0.33	0.27
0020	0.32	0.41
		R = 0.22

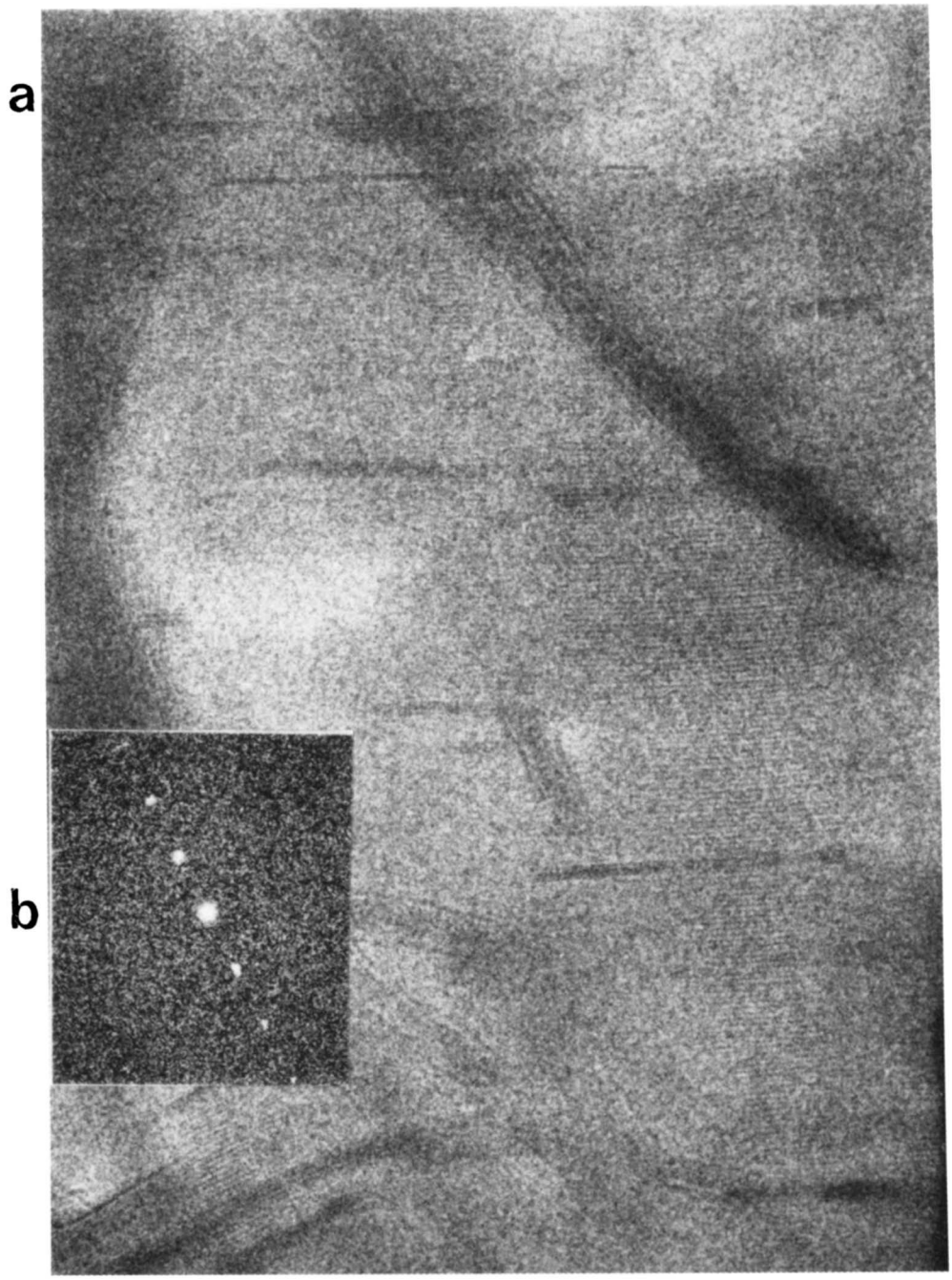

Fig. 3. (a) Low-dose electron microscope "lattice images" from epitaxially-grown cholesteryl myristate lath crystals. (There are no staining or embedding procedures in the sample preparation.) The lamellar repeat represents d_{002} ≈ 50 Å and from the optical transform of the image (b), the maximum resolution is 17 Å. Although bend-induced undulations are noted in the crystal, the lamellar lines are found to be very straight, unlike the case for phosphatidylethanolamines where these can be significantly curved (J. R. Fryer and D. L. Dorset, unpublished data). Thus, although some arcing of electron diffraction spots is noted below the pre-smectic transition crystal packing is formed, this is merely due to misorientation of adjacent crystallites within the selected area aperture of the electron microscope. To our knowledge, this is only the second lattice image of this type ever reported in the literature, the first one being of a epitaxially crystallized paraffin (37).

peak at a different spacing. Wendorff and Price (12) found no evidence for a pretransition crystal form and suggested that the sudden transition to the smectic phase probably is accompanied by a slip along the molecular long axes such that cholesterol nuclei in the smectic layers are surrounded by acyl chains. Craven and DeTitta (15) argued that, since there are many interatomic vectors near 33 Å for a molecular pair in the asymmetric unit of their crystal

structure, there could be average nematic-type shears of molecular pairs which nevertheless retain their mutual spacing. Thus, the continuous diffraction maximum would remain centered around this value. This would call for a more disordered layer structure than proposed by Wendorff and Price (12). In a recent report on a similar material, which also gave a smectic diffraction pattern with only one strong low angle peak, other workers (27) argued for a structural model somewhere between the two extremes suggested above.

From our electron diffraction data, we can make strong arguments for the existence of a pretransition crystal form, although it is not obvious from just the (00ℓ) diffraction data what this structure might be. After tilting the molecular axes normal to the layer surface, translation of one molecule versus the other in the associated pair described by Craven and DeTitta gives the best agreement with lamellar diffraction intensities from the pretransition form at a molecular shift only slightly away from the position found in the crystal structure, thus maintaining the layer thickness as found in our experiments. [Again, the apparent ordering of the specimen probably denotes the fusion of all adjacent crystallites into a continuous plastic crystal, as also indicated by their behavior in the light microscope (6).] However, since there is only one diffraction peak at 33 Å, the structural change responsible for the pretransition crystal form disordering into the smectic phase is not obvious. It is noted, however, that this peak is very sharp, both when it co-exists with the pretransition crystal form (Fig. 2) and after the transition. Sampling the continuous transform for molecular pairs with a 33 Å lattice spacing at various intermolecular shifts indicates various translation values where the first smectic intensity would be very strong compared to the second and third maxima, including positions where the cholesterol nuclei are packed with the long chains. Since the smectic reflection is very sharp (such that the effective shape function of the coherently scattering unit includes several layers), it is unlikely that a disordered packing of the type originally suggested by Craven and DeTitta (15), i.e., a smectic layer composed of nematically shifted dimer units, is an adequate model for this phase. Using arguments based on the theory of paracrystalline arrays (28, 29), it can be shown that the condition for one major reflection from a 33 Å repeating layer structure is that the molecular translational disorder must be less than 7.3 Å. At this limit, the broadening of the first diffraction peak would be 0.015 $Å^{-1}$ (corresponding to two coherently scattering units if such broadening is interpreted in terms of an Ewald shape function). These values follow from the minimum requirement for a single diffraction peak (29), i.e.,

$$\ell\Delta/c \approx 0.22 \qquad \textit{Eq. 1)}$$

and the half width ΔZ of the diffraction maximum at Miller index ℓ (28), i.e.,

$$\Delta Z = \frac{1}{c}\,\pi^2\ell^2\left(\frac{\Delta}{c}\right)^2.$$

Here Δ denotes the translational disorder of the scattering units and c is the lamellar repeat.

Since the disappearance of higher order reflections due to paracrystalline disorder leads to peak broadening, such an interpretation is thus contradicted by our observations. Even if the conditions for observed reflections in equation 1 allows for more peaks, e.g., a value of 0.18, the corresponding Δ = 5.9 Å leads to a peak width of 0.010 $Å^{-1}$. [It should also be pointed out that the peak broadening found for X-ray powder data was attributed to *lateral,* not longitudinal, disorder by Wendorff and Price (12).] Alternative models based on the crystal structure and also satisfying the molecular orientation of smectic A (27), e.g., which account for a hydrocarbon chain shortening upon melting [see Vand's work on n-hexatriacontane (30)], also would not account for the 17 Å shrinkage of the unit cell. Thus some sort of molecular translation along the long axes is indicated for the smectic transition. That the second and third diffraction peaks are weak in comparison to the first appears to be only a feature of the liquid crystal structure and does not necessarily signify a nematic disorder of the layer structure. However, attempts to satisfy this condition solely by longitudinal molecular displacement may also be overly simplistic, since the pretransition effects denote other intramolecular disorder mechanisms (e.g., kinks, end plane voids) which may also alter these reflections [e.g., see earlier work on paraffins (16)].

Similar conclusions have been reached recently by Sawzik (31) and Sawzik and Craven (32). As pointed out (31, 32), the lamellar spacing of numerous cholesteryl esters in the smectic phase corresponds well to the d_{001} spacing of a monolayer I crystal packing, which also accounts for the weak $I_{00\ell}$ for $\ell \geq 2$ discussed above. This model includes a 64° molecular tilt but, according to the diffuse cone model of DeVries (33), either smectic A or C texture could be produced by the molecular aggregation. (For a smectic A structure in DeVries' scheme, only the *average* molecular tilt needs to be orthogonal.) Although the retention of tilted molecular packing contradicts our supposition above of a structure in the pretransition crystal form with perpendicular molecular long axes, there are again too few lamellar data from such a complicated molecule to identify any particular structure unequivocally [see, for example, the significance test for R-values in Hamilton's book (34)]. From our data we can only declare that a pretransition crystal form does exist. It also appears that some sort of interpenetrated molecular packing is required for the smectic phase.

Transition from the smectic to the cholesteric phase remains undefined. Various workers indicate that some sort of smectic layering remains in this phase for cholesteryl esters (12, 35) a feature that could be accounted for

by the layer twisting found in spherulites, particularly since the cholesteric twist axes lie normal to the molecular long axis (36). However, the significance of angular crystallite displacements perpendicular to this direction when the material is cooled from the cholesteric is not yet understood and will be the subject of future investigations.

The author is grateful to Drs. B. M. Craven, P. J. Sawzik, and G. T. DeTitta for discussion of this work and to Mr. E. L. Hurley for technical assistance. Research was funded by Grant GM21047 from the National Institute of General Medical Science.

Manuscript received 13 February 1985.

REFERENCES

1. Small, D. M. 1970. The physical state of lipids of biological importance: cholesteryl esters, cholesterol, triglyceride. *Adv. Exp. Med. Biol.* **1:** 55–64.
2. Bergmann, K., and H. Stegemeyer. 1979. Evidence for polymorphism within the so-called "blue-phase" of cholesteric esters. I. Calorimetric and microscopic measurements. *Z. Naturforsch.* **34a:** 251–252.
3. Bergmann, K., P. Pollman, G. Scherer, and H. Stegemeyer. 1979. Evidence for polymorphism within the so-called "blue-phase" of cholesteric esters. II. Selective reflection and optical rotatory dispersion. *Z. Naturforsch.* **34a:** 253–254.
4. Bergmann, K., and H. Stegemeyer. 1979. Evidence for polymorphism within the so-called "blue-phase" of cholesteric esters. IV. Temperature and angular dependence of selective reflection. *Z. Naturforsch.* **34a:** 1031–1033.
5. Kuczynski, K., K. Bergmann, and H. Stegemeyer. 1980. A model of the blue phase of cholesteryl esters. *Mol. Cryst. Liq. Cryst.* **56:** 283–287.
6. Kunihisa, K. S., and T. Shinoda. 1975. Studies of phase transitions in cholesteryl myristate by means of simultaneous measurements of polarizing microscopy and thermal analyses. *Bull. Chem. Soc. Japan.* **48:** 3506–3511.
7. Barrall, E. M., R. S. Porter, and J. F. Johnson. 1967. Heats of transition for some cholesteryl esters by differential scanning calorimetry. *J. Phys. Chem.* **71:** 1224–1228.
8. Barrall, E. M., R. S. Porter, and J. F. Johnson. 1967. Specific heats of nematic, smectic, and cholesteric liquid crystals by differential scanning calorimetry. *J. Phys. Chem.* **71:** 895–900.
9. Davis, G. J., R. S. Porter, and E. M. Barrall. 1970. Evaluation of thermal transitions in some cholesteryl esters of saturated aliphatic acids. *Mol. Cryst. Liq. Cryst.* **10:** 1–19.
10. Price, F. P., and J. H. Wendorff. 1971. Transitions in mesophase forming systems. I. Transformation kinetics and pretransition effects in cholesteryl myristate. *J. Phys. Chem.* **75:** 2839–2849.
11. Wendorff, J. H., and F. P. Price. 1973. An X-ray diffraction study of crystalline cholesteryl myristate and cholesteryl stearate. *Mol. Cryst. Liq. Cryst.* **22:** 85–97.
12. Wendorff, J. H., and F. P. Price. 1973. The structure of mesophases of cholesteryl esters. *Mol. Cryst. Liq. Cryst.* **24:** 129–144.
13. McMillan, W. L. 1971. X-ray scattering from liquid crystals. I. Cholesteryl nonanoate and myristate. *Phys. Rev. A.* **6:** 936–947.
14. Burks, C., and D. M. Engelmann. 1981. Cholesteryl myristate conformation in liquid crystalline mesophases determined by neutron scattering. *Proc. Natl. Acad. Sci. USA.* **78:** 6863–6867.
15. Craven, B. M., and G. T. DeTitta. 1976. Cholesteryl myristate: structures of the crystalline solid and mesophases. *J. Chem. Soc. Perkin Trans.* **II:** 814–822.
16. Dorset, D. L., B. Moss, J. C. Wittmann, and B. Lotz. 1984. The pre-melt phase of n-alkanes: crystallographic evidence for a kinked chain structure. *Proc. Natl. Acad. Sci. USA.* **81:** 1913–1917.
17. Dorset, D. L., W. A. Pangborn, and A. J. Hancock. 1983. Epitaxial crystallization of alkane chain lipids for electron diffraction analysis. *J. Biochem. Biophys. Methods.* **8:** 29–40.
18. Wittmann, J. C., A. M. Hodge, and B. Lotz. 1983. Epitaxial crystallization of polymers onto benzoic acid: polyethylene and paraffins, aliphatic polyesters, and polyamides. *J. Polym. Sci. Polym. Phys. Ed.* **21:** 2495–2509.
19. Cowley, J. M. 1961. Diffraction intensities from bent crystals. *Acta Crystallogr.* **14:** 920–927.
20. Dorset, D. L. 1980. Electron diffraction intensities from bent molecular organic crystals. *Acta Crystallogr.* **A36:** 592–600.
21. Moss, B., and D. L. Dorset. 1983. Dynamical electron diffraction from elastically bent organic crystals. *Acta Crystallogr.* **A39:** 609–615.
22. Cowley, J. M., and A. F. Moodie. 1962. The scattering of electrons by thin crystals. *J. Phys. Soc. Japan.* **17 (suppl. B-II):** 86–91.
23. Doyle, P. A., and P. S. Turner. 1968. Relativistic Hartree-Fock X-ray and electron scattering factors. *Acta Crystallogr.* **A24:** 390–392.
24. Amoros, J. L., and M. Amoros. 1968. Molecular Crystals: Their Transforms and Diffuse Scattering. John Wiley & Sons, Inc., New York. 175–182.
25. Moss, B., D. L. Dorset, J. C. Wittmann, and B. Lotz. 1985. Quantitative analysis of electron diffraction data from epitaxially grown crystals. *J. Macromol. Sci. Phys.* In press.
26. Westrum, E. F., and J. P. McCullough. 1963. Thermodynamics of crystals. *In* Physics and Chemistry of the Organic Solid State. D. Fox, M. M. Labes, and A. Weissburger, editors. Wiley-Interscience, New York. 1–178.
27. Radzhabova, Z. B., V. A. Gudkov, S. P. Chumakova, and I. G. Chistyakov. 1983. Structural features of bilayer smectics-A. *Sov. Phys. Crystallogr.* **28:** 573–575.
28. Vainshtein, B. K. 1966. Diffraction of X-Rays by Chain Molecules. Elsevier, Amsterdam. 216–229.
29. Guinier, A. 1963. X-Ray Diffraction in Crystals, Imperfect Crystals and Amorphous Bodies. Freeman, New York. 297–304.
30. Vand, V. 1953. Density and unit cell of n-hexatriacontane. *Acta Crystallogr.* **6:** 797–798.
31. Sawzik, P. J. 1984. Crystal structures of cholesteryl esters. Ph.D. thesis, University of Pittsburgh.
32. Sawzik, P., and B. M. Craven. 1980. Cholesteryl esters: crystal and mesophase structures. *In* Proc. Internatl. Conf. on Liquid Crystals, Bangalore, India. S. Chandrasekhar, editor. Heyden & Sons, Philadelphia. 171–178.
33. DeVries, A. 1980. Structure and symmetry of smectic liquid crystals. *In* Advances in Liquid Crystal Research and

Applications. L. Bata, editor. Pergamon Press, Oxford. 71–80.
34. Hamilton, W. C. 1964. Statistics in Physical Science. Estimating, Hypothesis Testing and Least-Squares. Ronald Press Co., New York. 157–162.
35. Chistyakov, I. G. 1964. The structure of n,n′ non-oxybenzal toluidine and cholesteryl caprate in the liquid-crystal state. *Sov. Phys. Crystallogr.* **8:** 691–694.
36. Voss, J., and B. Voss. 1976. SEM studies of cholesteric liquid crystals. *Z. Naturforsch.* **31a:** 1661–1663.
37. Fryer, J. R. 1981. Lattice imaging of radiation-sensitive materials. Inst. Phys. Conf. Ser. No. 61. 15–22.